

Experimental studies of circular composite bridge piers for seismic loading

Sheng-Jin Chen¹, Kuo-Chen Yang^{*2}, K.M. Lin¹ and C.C. Wang¹

¹National Taiwan University of Science and Technology, Department of Construction Engineering, Taipei, Taiwan

²National Kaohsiung First University of Science and Technology, Department of Construction Engineering, Kaohsiung, Taiwan

(Received March 18, 2011, Revised October 11, 2011, Accepted January 13, 2012)

Abstract. This study proposes and examines a circular composite bridge pier for seismic resistance. The axial and flexural strengths of the proposed bridge pier are provided by the longitudinal reinforcing bars and the concrete, while the transverse reinforcements used in the conventional reinforced concrete pier are replaced by the steel tube. The shear strength of this composite pier relies on the steel tube and the concrete. This system is similar to the steel jacketing method which strengthens the existing reinforced concrete bridge piers. However, no transverse shear reinforcing bar is used in the proposed composite bridge pier. A series of experimental studies is conducted to investigate the seismic resistant characteristics of the proposed circular composite pier. The effects of the longitudinal reinforcing bars, the shear span-to-diameter ratio, and the thickness of the steel tube on the performance of strength, ductility, and energy dissipation of the proposed pier are discussed. The experimental results show that the strength of the proposed circular composite bridge pier can be predicted accurately by the similar method used in the reinforced concrete piers with minor modification. From these experimental studies, it is found that the proposed circular composite bridge pier not only simplifies the construction work greatly but also provides excellent ductility and energy dissipation capacity under seismic lateral force.

Keywords: composite bridge pier; ductility; steel tube; seismic resistance

1. Introduction

Bridge piers are the essential load-carrying members of a bridge system. To ensure sufficient strength and ductility of a circular reinforced concrete pier under seismic load, sufficient transverse reinforcements are needed as following (ATC 1996, AASHTO 2008, ACI 2008)

$$\rho_s \geq 0.45 \left(\frac{A_g}{A_c} - 1 \right) \frac{f_c'}{f_{yh}} \left(0.5 + 1.25 \frac{P_e}{f_c' A_g} \right) \quad (1)$$

or

$$\rho_s \geq 0.12 \frac{f_c'}{f_{yh}} \left(0.5 + 1.25 \frac{P_e}{f_c' A_g} \right) \quad (2)$$

* Corresponding author, Ph.D., E-mail: kcyang@nkfust.edu.tw

Where ρ_s is the transverse reinforcement ratio used; A_g is the gross sectional area of the pier (cm^2); A_c is the cross-sectional area of the concrete core (cm^2); f_c' is the specified compressive strength of the concrete (MPa); and f_{yh} is the yield stress of the reinforcing bars (MPa), and P_e is the axial load (kN). The spacing of the transverse reinforcement is limited to one-quarter of the minimum dimension of the cross section or 15 cm center-to-center distance of the transverse reinforcements, but not less than 10 cm to prevent buckling of the longitudinal reinforcement bars (AASHTO 2008, ACI 2008). Sufficient strength and ductility of the reinforced concrete pier can be achieved with these transverse requirements. However, the closely spaced transverse reinforcements may interfere the casting of concrete and increase the construction cost.

This study examines the behavior of a new circular composite bridge pier system. The proposed composite pier is similar to the steel jacketing system used in strengthening of the existing RC piers (Chai *et al.* 1991, Priestley *et al.* 1994a, Priestley *et al.* 1994b, Aboutaha 1999a), which the steel tube is used to enhance shear strength and ductility of the bridge piers. The major difference between the proposed system and the steel jacketing method is the absence of the transverse reinforcement in the proposed composite pier construction. The concept of the steel jacketing system has not been adopted in designing new bridge piers. The proposed composite pier is also similar to the concrete-filled tubular (CFT) pier (Aboutaha 1999b, Ellobody *et al.* 2006, Gupta *et al.* 2007, Chitawadagi *et al.* 2009, Lee *et al.* 2009, Roeder *et al.* 2010), except the steel tube of the composite pier is not anchored to the foundation and does not share the resistance of the flexural moment or the axial load. This is done by providing a gap of 5 cm between the steel tube and the foundation. This gap is to avoid direct bearing of the steel tube on the foundation. However, if the gap is too large, premature spalling of the concrete and buckling of the longitudinal reinforcing bar may occur. The empirical value of 5 cm follows the design guidelines used in the concrete pier design as the first stirrup is usually 5 cm away from the top of the foundation. The steel tube is not required to connect to the foundation, since it does not contribute to the flexural resistance. With this arrangement, the complicated construction work required for the anchorage of the steel tube to the concrete foundation can be avoided. The axial and flexural strength of this composite pier are provided by the longitudinal reinforcing bars and the concrete.

The proposed composite bridge pier adopts both advantages of the reinforced concrete and the steel tube. Meanwhile, the proposed method also avoids complicated construction work in the conventional RC column or CFT column. The possible defect due to closely spaced transverse reinforcements or welding of steel tube to the anchor frame can be avoided. The steel tube provides shear resistance and confines the concrete, which enhances the strength and deformation capacity of bridge pier. The steel tube also serves as the formwork for the concrete casting. Fig. 1 shows the schematic drawing of the proposed composite pier. The application of this method to the rectangular composite pier system is discussed in reference (Chen *et al.* 2011). Excellent performance of the rectangular composite pier under seismic load is also observed.

2. Theoretical background

In the proposed circular composite bridge piers, the axial and flexural strengths of this composite pier are provided by the reinforced concrete columns and are determined to be identical to the conventional method used in the design of reinforced concrete columns (ACI 2008). The nominal shear strength of the composite pier (V_n) can be obtained by summing the strengths contributed from the steel tube (V_s) and the concrete (V_c) as follows

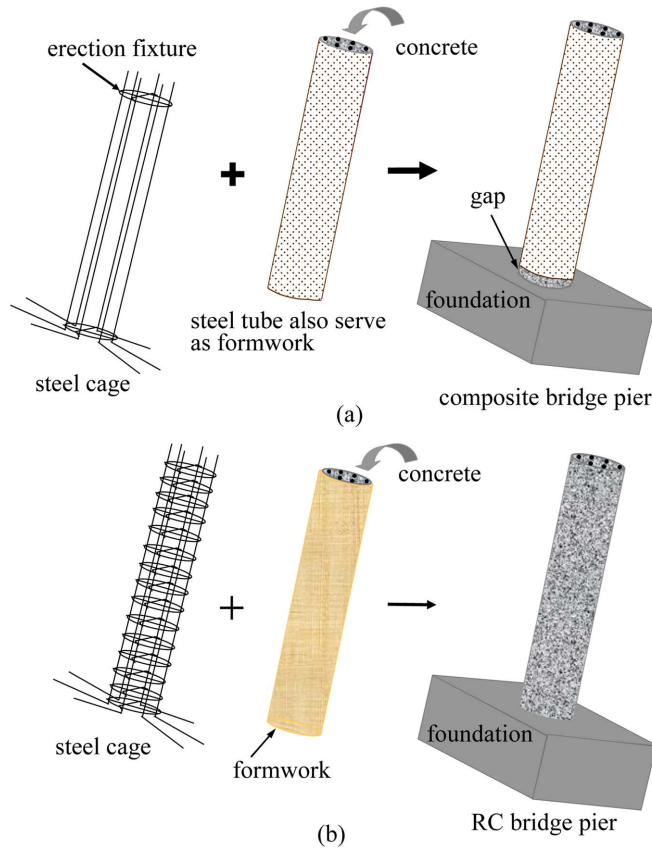


Fig. 1 Schematic of the bridge pier system: (a) proposed composite bridge pier system; (b) conventional reinforced concrete bridge system

$$V_n = V_c + V_s \quad (3)$$

The behavior of the confined concrete has been studied extensively and the stress-strain models are well-established, which include the concrete confined by the transverse reinforcements for the conventional reinforcement concrete piers and concrete confined by the steel tube for the CFT columns (Park *et al.* 1982, Sheikh *et al.* 1982, Mander *et al.* 1988a, Mander 1988b, Hoshikuma *et al.* 1997). In general, the shear strength carried by the confined concrete can be calculated as follows (ACI 2008)

$$V_c = \alpha \left(1 + \frac{P}{140A_g} \right) \sqrt{f'_c} \cdot A_e \quad (4)$$

In Eq. (4), α is the coefficient of shear strength of the confined concrete depending on the confinement, $\alpha = 0.17 \sim 0.29$ (ACI 2008); f'_c is the specified concrete compressive strength (MPa); A_g is the gross sectional area of the pier (cm^2); A_e is the effective cross sectional area for shear resistance (cm^2); and P is the axial compressive load (kN). The steel tube provides better confinement to the concrete and enhances the shear resistance of the concrete. In this pilot study, the enhanced shear resistance from the confinement by the steel tube is neglected and a conservative value of $\alpha = 0.29$ is suggested to calculate

the shear resistance of the concrete in Eq. (4). The shear strength provided by the steel tube can be determined as following (Ghee *et al.*1989, Priestley *et al.*1994c)

$$V_s = \frac{\pi}{2} t_s F_y D \cot \theta \quad (5)$$

In Eq. (5), t_s is the thickness of the steel tube; F_y is the yield strength of the steel tube; D is the diameter of the bridge pier; and θ is the inclined angle of the crack. In the design of bridge pier, the design shear strength $\phi_s V_n$ should be larger than maximal factored load V_u . The required tube thickness can be determined as shown in Eq. (6).

$$t_s = \left(\frac{V_u}{\phi} - V_c \right) \frac{2}{\pi F_y \cot \theta} \quad (6)$$

3. Experimental study of circular composite bridge piers

To evaluate the performance of the proposed circular composite bridge pier, a series of experimental work has been carried out in this study. Five specimens were tested under monotonic load and two specimens were subjected to cyclic loads (Table 1). With the identical dimensions and tube thickness, the designed shear strengths (V_n) of specimens under monotonic load (Specimens STC1 ~ STC5), were the same. However, the ultimate strengths of the specimens were governed by shear failure ($V_u / V_n > 1.0$), flexural-shear failure ($V_u / V_n \approx 1.0$), and flexural failure ($V_u / V_n < 1.0$) by varying the longitudinal reinforcement ratios and span-to-diameter ratios. The smaller span-to-diameter ratios were selected to simulate the most rigorous situation of bridge piers under seismic loads. The shear span-to-diameter ratio is the shear span, a , divided by the diameter of the specimen, d , as shown in Fig. 2. The specimens were loaded by two-point loads so that the loading condition of the specimen on both sides is similar to the cantilever bridge pier subjected to lateral load. At the loading point, the specimen is strengthened to simulate the bridge foundation. Specimens CC1 and CC2 are designed to investigate the behavior of composite bridge under cyclic load (Fig. 3). Strain gages were used to monitor the strains on the reinforcing bars and the steel tube. Linear variation displacement transducers (LVDT) were installed to measure the displacement of the specimens. Table 1 summarizes the parameters used in designing of these specimens. The material properties of concrete, reinforcing bars and steel tubes are listed in Table 2.

3.1 Behavior of composite piers under monotonic load

The fundamental behaviors of the proposed composite piers were examined under monotonic load. Specimens STC1 - STC2 with a smaller span-to-diameter ratio of 1.55, are designed to examine the shear failure mode of the bridge pier under seismic loads. Specimens STC3 - STC5 were aimed at examining the performance of the composite pier with a larger span-to-diameter ratio of 1.78. These specimens were tested under combined shear and flexure forces. Table 3 lists a summary of the parameters examined in this study and the results of the composite piers under monotonic loads. The designed flexural moment (M_n) is determined based on current bridge design specification (AASHTO 2008). The design strengths listed in Table 3 are obtained according to the actual material strengths listed in Table 2. The ratios of V_u / V_n that based on the nominal strength are also included in Table 3.

Table 1 Design parameters of bridge pier specimens

Specimens	Loading type	Diameters, d (cm)	Steel tube		Reinforcement ratio, ρ_s	Shear span, a (cm)	Specimen length, L (cm)
			Thickness, t_s (mm)	Length, S (cm)			
STC1	Monotonic load	45	2	54	-	70	230
STC2		45	2	54	-	70	230
STC3		45	2	64	-	80	250
STC4		45	2	64	-	80	250
STC5		45	2	64	-	80	250
CC1	Cyclic load ⁽¹⁾	50	3	212	4 × 7 @30 cm	250	335
CC2		50	6	212	4 × 7 @30 cm	250	335

Notes: (1) with axial compressive force of $0.07 f_c' A_g = 490$ kN; (2) the longitudinal reinforcement is #8 with a diameter of 25 mm

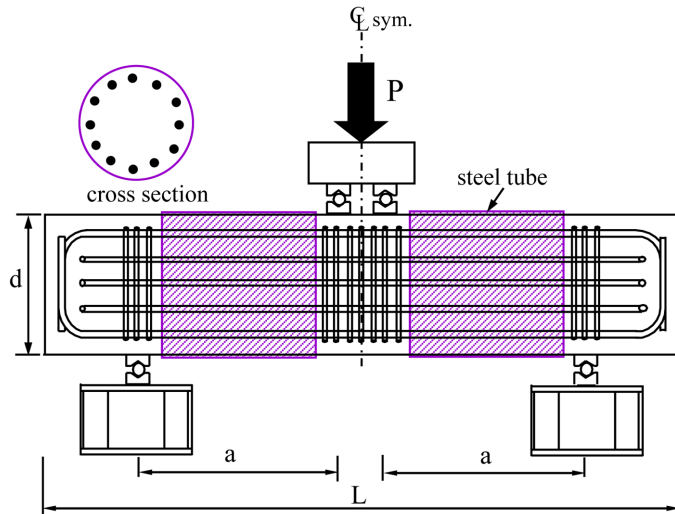


Fig. 2 Test set-ups of bridge pier specimens under monotonic loads

3.1.1 Load-displacement relationships of specimens under monotonic load

The load-displacement relationships of Specimen STC1~STC2 are shown in Fig. 4. Excellent strength and deformation capacity were observed from these studies. Specimens retained at least 85% of their ultimate strength even the displacement ductility factors have exceeded 10. The strains of the longitudinal reinforcements exceeded $5 \epsilon_y$ and $9 \epsilon_y$ as Specimens STC1 and STC2 reached their ultimate strengths, in which ϵ_y is the yield strain of the longitudinal reinforcement. Specimens STC1 and STC2 failed due to the fracture of the longitudinal reinforcements and crushing of the concrete.

Fig. 5 shows the load-displacement relationships of Specimens STC3 - STC5. Specimen STC3 retained its strength with large plastic deformation after the concrete crushed. The displacement ductility ratio (μ) of Specimen STC3 was 5.1 and retained more than 80% of its ultimate strength. At the final stage, longitudinal steel bars reach a strain of $4 \epsilon_y \sim 10 \epsilon_y$, as shown in the strain reading 1 and 3 in Fig. 6(b). A strain of $5 \epsilon_{y, st}$ in the circumferential direction was also measured in the steel tube at the ultimate stage

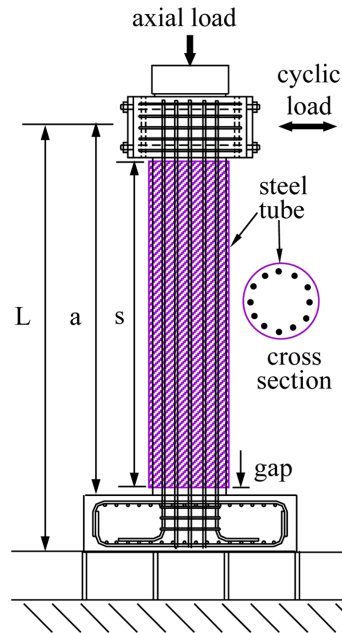


Fig. 3 Test set-ups of bridge pier specimens under cyclic loads

Table 2 Material properties of the specimens

Specimens	f'_c	f_{ys}	F_y
STC1	57	432	330
STC2	54	432	330
STC3	58	432	330
STC4	55	432	330
STC5	58	432	330
CC1	37	421	245
CC2	36	421	265

f'_c : is the actual concrete compressive cylinder strength (MPa);

f_{ys} : is the yield stress of longitudinal reinforcements (MPa);

F_y : is the yield strength of steel tube (MPa);

The nominal strength for concrete, longitudinal reinforcements and steel tube is 34.3 MPa, 412 MPa and 245 MPa, respectively.

(Fig. 6), in which $\varepsilon_{y, st}$ is the yield strain of the steel tube. Because the steel tube was designed to share shear strength without taking flexural moment and axial load, the strain on the steel tube was approximately zero in the longitudinal direction (Strain reading 5 in Fig. 6(c)). A significant yielding and dilation were observed (Fig. 7) with a measured strain of 0.004 in the direction of 45° on steel tube (Strain reading 6 in Fig. 6(c)). This not only demonstrated that the steel tube provide excellent confinement to the concrete but also showed that the composite action exists between steel tube and the concrete.

Specimens STC3, STC4 and STC5 are aimed to examine the effect of the amount of longitudinal reinforcements. The flexural induced shear force decreased with the reduction of longitudinal reinforcements. Increase in displacement ductility ratios of 4.1 to 12.5 were observed as the longitudinal reinforcements

Table 3 Summary of design parameters and test results for bridge pier specimens

Specimens	Specimen details		Calculated strengths						$\frac{V_n^*}{V_n}$	P_{cal} kN	P_{exp} kN	$\frac{P_{exp}}{P_{cal}}$	$\frac{P_{exp}}{P_{AISC}}$	μ (D_m/D_y)	$\frac{ED_{max}}{ED_{yield}}$
	$\frac{\text{shear span}}{\text{diameter}}$	tube thickness	M_n kN-m	V_s kN	V_c kN	V_n kN	$\frac{V_u}{V_n}$								
STC1	1.55	2 mm	597	467	355	822	1.04	1.22	853	1094	1.28	2.34	4.1	8.5	
STC2	1.55	2 mm	484	467	346	812	0.85	0.96	691	979	1.42	2.10	5.6	11.5	
STC3	1.78	2 mm	597	467	358	825	0.90	1.04	746	987	1.32	2.11	5.1	12.9	
STC4	1.78	2 mm	538	467	349	817	0.83	0.93	673	916	1.36	1.96	9.5	14.2	
STC5	1.78	2 mm	369	467	358	825	0.56	0.61	461	564	1.22	1.22	12.5	19.4	
CC1	5.55	3 mm	572	577	353	931	0.25	0.25	229	244	1.07	1.07	6.2	9.2 [†]	
CC2	5.55	6 mm	624	1249	348	1597	0.16	0.16	250	279	1.12	1.12	10.8	22.8 [†]	

V_n : shear strength for pier specimen; V_c : shear strength of concrete, assuming $\alpha = 0.29$ in Eq. (3); V_u : shear force induced by the designed flexural moment(= M_n / a); V^* : shear strength based on nominal material strengths; P_{cal} : design strength of specimens based on the real material properties; P_{exp} : maximum lateral force derived from the experimental works; P_{AISC} : calculated strength based on AISC; μ : displacement ductility factor (= D_m / D_y); D_m : displacement corresponding to the ultimate shear strength; D_y : displacement corresponding to the yielding strength; ED_{max} : energy dissipation under the maximum load (P_{exp}) and its corresponding displacement (D_m); ED_{yield} : energy dissipation under the yield load (P_y) and its corresponding displacement (D_y); [†]: based on the envelope of the hysteresis curves for specimen under cyclic loads.

reduced from 5.1% of Specimen STC3 to 1.91% of Specimen STC5. The strength degradation of Specimen STC5 was less than 5% when reached a displacement ductility ratio of 12.5. Specimen STC5 failed due to the fracture of longitudinal reinforcement at a drift ratio of 22%. With smaller amount of longitudinal bars used in Specimen STC5 as compared with STC3, the deformation capacity of STC5 was greatly enhanced. It was noted that although no shear studs were used for specimens tested under monotonic load, the composite pier demonstrated good strength and ductility. The effect of shear studs

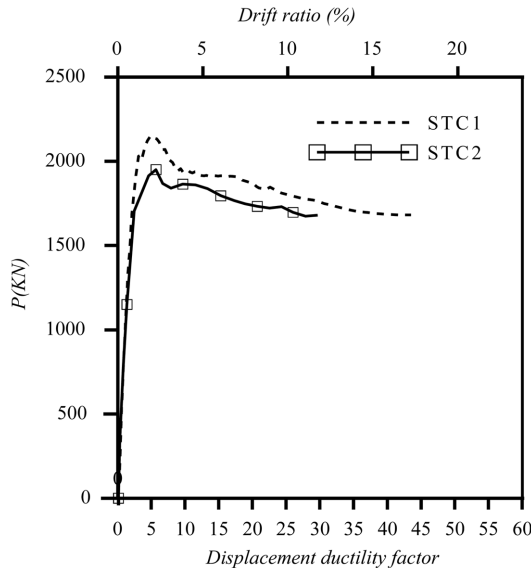


Fig. 4 Load-displacement relationship of specimens STC1 ~ STC2

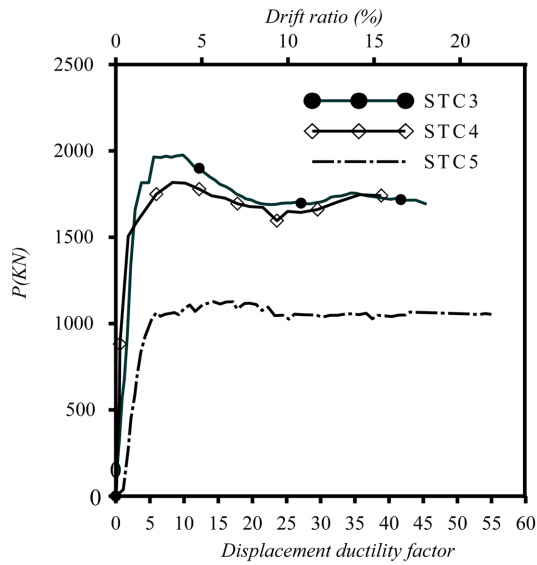


Fig. 5 Load-displacement relationship of Specimens STC3 ~ STC5

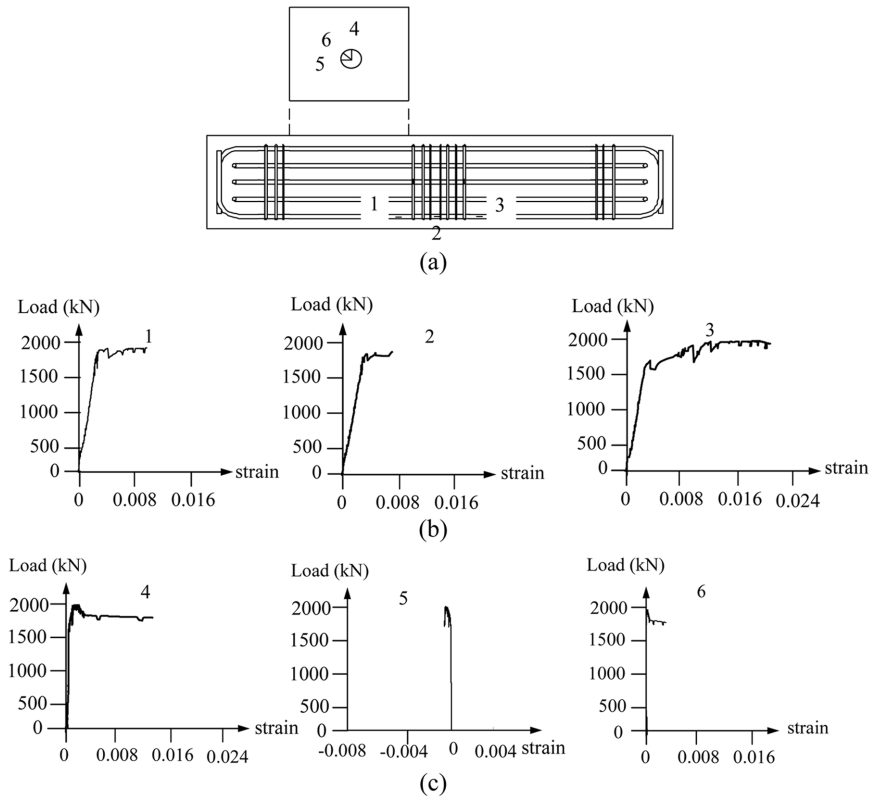


Fig. 6 Typical stresses distribution on the webs of specimens under monotonic load (Specimen STC3): (a) gage position; (b) strain on longitudinal steel bars; (c) strains on steel tube.

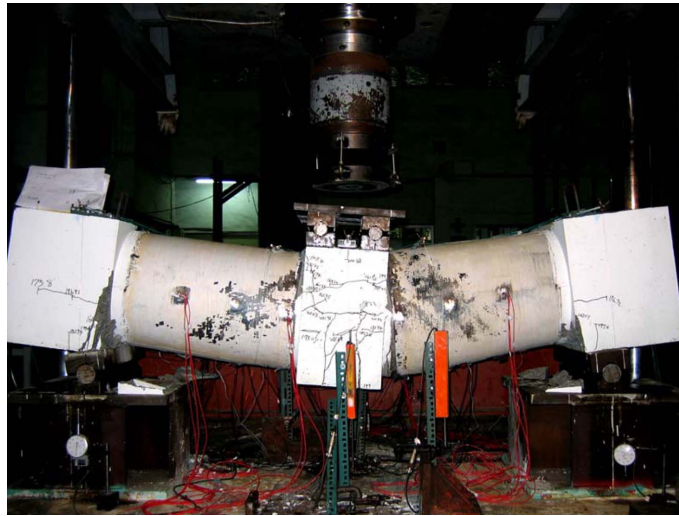


Fig. 7 Typical failure mode of composite bridge piers (specimens STC3)

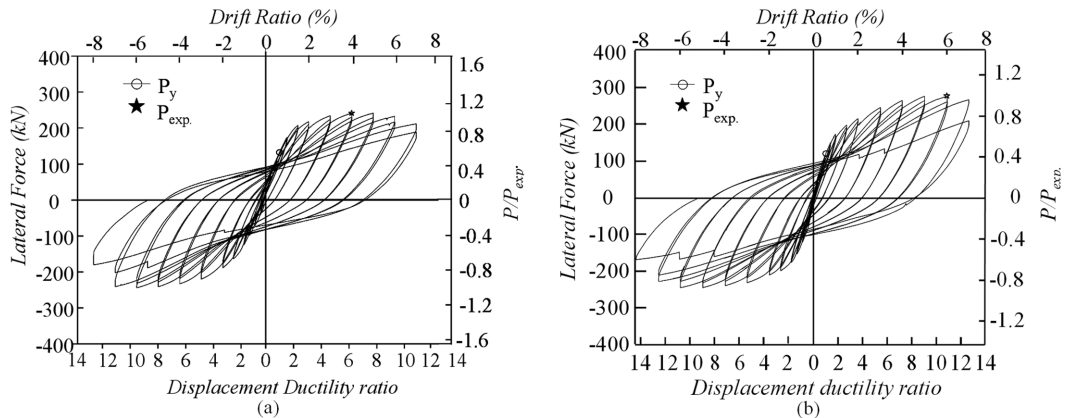


Fig. 8 Hysteresis behavior of composite pier: (a) tube thickness = 3 mm; (b) tube thickness = 6 mm

has been discussed in the rectangular composite bridge pier (Chen *et al.* 2011) and in the specimens under cyclic load.

From the experimental results, it was also found that the simplified equations (Eqs. (3)~(6)) provided a conservative value for the calculation of the ultimate strength of the composite circular bridge piers. It is shown in Table 3 that the ratio of tested strengths (P_{exp}) to the calculated strengths (P_{cal}) based on Eqs. 3~5 are 1.07 ~ 1.42, with an average value of 1.26. The variations between the calculated strengths and the experimental strengths are mainly due to the simplified empirical confinement coefficient used in Eq. 4. The method to predict the strength of composite column is also available in the design specification published by AISC (AISC 2005). However, the experimental strengths are about two times that of calculated strengths based on the AISC method if specimens failed in shear (Table 3). It is suggested to use Eqs. (3)~(6) for the strength calculation of the composite circular pier for the simplicity and accuracy.

3.1.2 Effect of shear ratio, V_u/V_n

The displacement ductility ratio of the composite specimen increased with the decrease of the shear force. The ductility of the specimen was greatly enhanced if the shear ratio was less than 1.0. With a smaller shear strength ratio, the ultimate strength of the composite pier is governed by its flexural strength. The shear strength ratio, V_u/V_n , is the ratio of the shear force induced by the flexural moment to the designed shear strength. A smaller shear ratio means that the pier is subjected to a larger flexural moment and a small shear force. A displacement ductility ratio of 4.1 was ensured even for specimens subjected to a larger shear force. In the seismic design of the bridge pier, a displacement ductility ratio of 2~4 is usually recommended (FHWA 1995). With the increase of the displacement ductility, the dissipated energy also increased. The energy dissipation ratio (ED_{max}/ED_{yield}) increases from 8 to 20 if the shear ratio is decreased from 1.04 to 0.56 (Table 3).

3.1.3 Effect of shear span-to-diameter ratio, a/d

The shear force induced by flexural moment decreased with the increase of shear span. The effect of shear span was expressed by the shear span-to-diameter ratio of the specimens. Both Specimens STC1 and STC3 have the same design strengths in shear and flexural moment. The shear span-to-diameter ratios for Specimens STC1 and STC3 were 1.56 and 1.78 respectively. With different shear span-to-diameter ratios, the displacement ductility was increased from 4.1 for Specimen STC1 to 5.1 for Specimen STC3. The energy dissipation capacity of Specimen STC3 was also larger than that of Specimen STC1 by more than 50% (Table 3). Specimens STC2 and STC4 were designed to have same shear strength ratio, V_u/V_n , but the shear span-to-diameter ratios for STC2 was 1.56 and 1.78 for STC4. The displacement ductility ratio of STC2 was 5.6 while STC4 was 9.5. For specimens having the same shear ratio, the composite pier with larger shear span-to-diameter ratio shows better ductile behavior. The proposed circular composite bridge pier is able to have a displacement ductility factor more than 4.0 even with very small shear span-to-diameter ratio.

3.2 Behavior of composite piers under cyclic load

The proposed composite bridge pier was further examined by applying the cyclic lateral load to the cantilever type bridge piers to examine the behavior of the composite column under recursion of cyclic load. The design of Specimens CC1 and CC2 were the same except that the steel tube thickness of Specimen CC1 was 3 mm while Specimen CC2 was 6 mm. This was to examine the effectiveness of the steel tube in the enhancement of shear strength and energy dissipation. Four shear studs with longitudinal spacing of 300 mm were added to Specimen CC1 and CC2 in order to ensure the integrity of the steel tube with the composite pier. Although the behavior of specimen under monotonic load could not be compared with that from cyclic load directly, the study of specimen under cyclic load provided valuable information on the strength, energy dissipation and hysteresis behavior of composite pier under recursion of lateral load.

An axial load about 10% of the axial compressive strength of the pier was applied to the specimen in order to simulate the concurrence of gravity load and seismic lateral load. The axial load usually induces second order effect during earthquake excitation. The second order effect accelerates the pinching effect of the reinforced concrete bridge pier under seismic load. However, the steel tube provides very good confinement to the concrete and alleviates the pinching effect of composite pier under cyclic load. Fig. 8 shows the hysteresis behavior of the composite bridge piers under combined axial and lateral load. The hysteresis behaviors shown in Fig. 8 indicated stable performance of the proposed bridge pier under

cyclic load. After reaching their ultimate states, the strengths of the specimens decreased gradually. The displacement ductility factors reached $\mu = \pm 6$ for specimen CC1 and $\mu = \pm 10$ for specimen CC2. The plastic hinges of the composite pier specimens had the length of 20 ~ 25 cm, which was about 40% ~ 50% of the diameter of the specimens. The plastic curvature of the section was about 0.35 ~ 0.40 (rad/m), as shown in Fig. 9. At the final stage, both specimens failed after the longitudinal reinforcing bars fractured (Fig. 10).

With the same design in flexural strength, the shear strengths of Specimens CC1 and CC2 were different. The thicknesses of steel tube used in Specimens CC1 and CC2 were 3 mm and 6 mm, respectively. The design shear strengths of Specimens CC1 and CC2 were 931 kN and 1,597 kN, as shown in Table 3. The 3 mm plate provided about 50% of shear strength for Specimen CC1; while, the 6 mm plate contributed 75% of the shear strength for Specimen CC2. From Table 3, it is shown that by increasing the tube thickness from 3 mm to 6 mm, the experimental ultimate strength of the Specimen CC1 and CC2 increased from 244 kN to 279 kN. It seemed that the ultimate strength of both specimens did not increase significantly by doubling the thickness of the tube, since the major function of the steel tube was to provide the shear strength in the pier. The increase of the ultimate flexural strength of the composite pier was due to the enhancement of confinement on the concrete. However, the displacement ductility ratio (μ) increased significantly from 6.2 to 10.8 with thicker tube used. The dissipated energy also increased from an energy ratio of 9.2 to 22.8 (E_{total} / E_{yield}) as shown in Table 3. The thicker tube was less prone to buckle, and was able to provide better confinement to the concrete and enhanced the energy dissipation capacity of the composite pier greatly.

4. Conclusions

The proposed circular composite bridge pier consists of a steel tube and an interior reinforced concrete

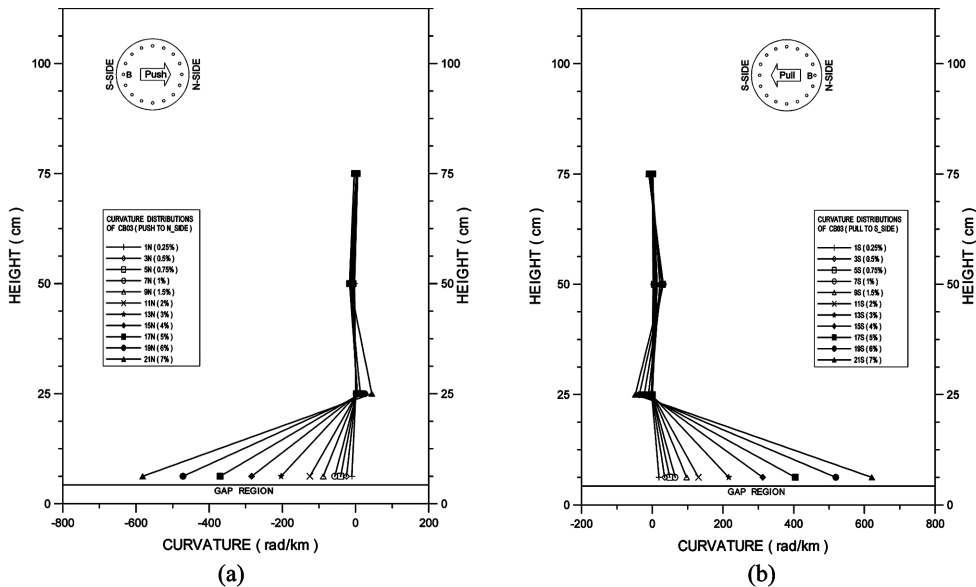


Fig. 9 Average curvature along the length of Specimen CR1: (a) push to the right; (b) pull to the left



Fig. 10 Fracture of reinforcing bars in the plastic hinge zone at the bottom of composite pier (Specimen CC1)

core. The reinforced concrete core provides the axial and flexural strengths of the bridge pier. The steel tube provides the shear resistance and confinement of the concrete to enhance the strength and ductility of the bridge pier. No transverse reinforcement is used, and the steel tube is not connected to the foundation. Experimental study shown that the displacement ductility factors obtained were 4.1-12.5 for the composite piers under monotonic load. For specimens under cyclic load, the displacement ductility factors were greater than 6 and the drift ratios were more than 4% without significant decay on the strength. The flexural strength of the proposed composite bridges pier can be accurately predicted following the same design method of the reinforced concrete bridge pier. While the shear strength of the proposed composite bridges pier can be obtained by the summation of the shear strengths from both the concrete core and the steel tube. Besides the enhancement on the strength and ductility, the construction works of the proposed method are greatly simplified as compare to the conventional reinforced concrete bridge piers. In the design of the tube thickness of the composite pier, it is suggested to adopt Eq. (4) for its simplicity. Further research is suggested to build an optimal design method for this type circular composite pier.

Acknowledgements

The research reported here is supported by the National Science Council of Taiwan under Grant NSC-95-2211-E011-196.

References

- AASHTO, (2008), *Standard Specifications for Highway Bridges-LRFD*. fourth edition, American Association of State Highway and Transportation Officials, Washington, D.C.
- Aboutaha, R.S. (1999a), "Rehabilitation of shear critical concrete columns by use of rectangular steel jackets", *ACI Struct. J.*, **96**(1), 68-78.
- Aboutaha, R.S. (1999b), "Seismic resistance of steel-tubed high-strength reinforced-concrete columns", *J. Struct. Engrg.*, *ASCE*, **125**(5), 485-494.
- ACI Committee 318 (2008), *Building Code Requirements for Structural Concrete and Commentary*, American Concrete Institute, Michigan.
- American Institute of Steel Construction, AISC (2005), *Specification for Structural Steel Buildings*, Chicago, IL.

- Applied Tech. Council, ATC (1996), *Improved Seismic Design Criteria for California Bridges: Provisional Recommendations*. ATC-32, Applied Tech. Council, Berkeley, Calif.
- Chai, Y.H, Priestley, M.J.N. and Seible, F. (1991), "Seismic retrofit of circular bridge columns for enhanced flexural moments", *ACI Struct. J.*, **88**(5), 572-584.
- Chen S.J., Yang K.C., Lin K.M. and Wang C.D. (2011), "Seismic behavior of ductile rectangular composite bridge piers", *Earthquake Engng Struct. Dyns.*, **40**(1), 21-34.
- Ellobody, E., Young, B. and Lam, D. (2006), "Behaviour of normal and high strength concrete-filled compact steel tube circular stub columns", *J. Constr. steel Res.*, **62**(7), 706-715.
- FHWA, (1995), *Seismic Retrofitting Manual for Highway Bridges*, FHWA-RD-94-052.
- Ghee, A.B., Priestley, M.J.N. and Paulay, T. (1989), "Seismic shear strength of circular reinforced concrete", *ACI Struct. J.*, 45-59.
- Gupta, P.K., Sarda, S.M. and Jumar, M.S. (2007), "Experimental and computational study of concrete filled steel tubular columns under axial loads", *J. Constr. steel Res.*, **65**(2), 182-193.
- Hoshikuma, J., Kawashima, K. and Taylor, A.W. (1997), "Stress-strain model for confined reinforced concrete in bridge piers", *J. Struct. Engrg., ASCE*, **123**(5), 624-633.
- Mander, J.B., Priestley, M.J.N. and Park, R. (1988a), "Observed stress-strain behavior of confined concrete", *J. Struct. Engrg., ASCE*, **114**(8), 1827-1849.
- Mander, J.B., Priestley, M.J.N. and Park, R. (1988b), "Theoretical stress-strain model for confined concrete" *J. Struct. Engrg., ASCE*, **114**(8), 1804-1826.
- Chitawadagi M.V. and Narasimhan M.C. (2009), "Strength deformation behavior of circular concrete filled steel tubes subjected to pure bending", *J. Constr. steel Res.*, **65**(8-9), 1836-1845.
- Lee E.T., Yun B.H., Shim H.I., Chang K.H. and Lee G.C. (2009), "Torsional behavior of concrete-filled circular steel tube columns", *J. Struct. Engrg., ASCE*, **135**(10), 1250-1259.
- Park, R., Priestley, M.J.N. and Gill, W.D. (1982), "Ductility of square-confined concrete columns", *J. Struct. Engrg., ASCE*, **108**(4), 929-950.
- Priestley, M.J.N., Seible, F., Xiao, Y. and Verma, R. (1994a), "Steel jacket retrofitting of reinforced concrete bridge columns for enhanced shear strength-Part 1: Theoretical considerations and test design", *ACI Struct. J.* **91**(4), 394-405.
- Priestley, M.J.N., Seible, F., Xiao, Y. and Verma, R. (1994b), "Steel jacket retrofitting of reinforced concrete bridge columns for enhanced shear strength-Part 2: Test results and comparison with theory", *ACI Struct. J.* **91**(5), 537-551.
- Priestley, M.J.N., Verma, R. and Xiao, Y. (1994c), "Seismic shear strength of reinforced concrete columns", *J. Struct. Engrg., ASCE*, **120**(8), 2310-2329.
- Roeder C.W., Lehman E.E. and Bishop E. (2010), "Strength and stiffness of circular concrete-filled tubes", *J. Struct. Engrg., ASCE*, **136**(12), 1545-1554.
- Sheikh, S.A. and Uzumeri, S.M. (1982), "Analytical model for concrete confinement in tied columns", *J. Struct. Engrg., ASCE*, **108**(12), 2703-2722.